Chiral Symmetry Breaking in Isotropic Liquids

[Widom symposium, ACS meeting, Washington, DC, Aug.20-24, 2017]

Abstract:
Given proper temperature and pressure conditions, a few substances display spontaneous formation of coexisting isotropic chiral liquids. This arises from preferred amorphous stacking geometries that are determined by the molecular shapes, by conformational flexibilities, and by intermolecular interactions that bias chiral inversion transitions. In order to investigate aspects of this phenomenon, a simple continuum tetrameric molecular model has been created and investigated both analytically and by computer simulation. One of the features that arises is the possible existence of two critical points, a conventional liquid-vapor separation for the racemic fluids, and a lower-temperature chiral symmetry breaking critical point above the freezing temperature. For some model interaction parameters one expects a confluence of these two critical points, raising questions about the resulting critical exponents. In order to amplify the characteristics of the tetramer model's interactions, ground-state crystal structures have been investigated for both enantiopure and racemic selections of the assigned interaction parameters.

It is a gratifying honor to contribute to this symposium recognizing Ben Widom's remarkable scientific career. The wide range of properties exhibited by liquids and their interfaces has provided basic motivation for his theoretical research, the results of which have had major impact. This area still presents many fascinating opportunities for future investigation, owing to the wide chemical and physical diversity of the substances exhibiting liquid phases. The present lecture considers one somewhat unusual portion of that general subject, specifically the occurrence of spontaneous chiral symmetry breaking within liquids that remain isotropic.

View 1. Title, coauthors, affiliations.

Isotropic chiral liquids that rotate polarized light can simply be formed as dilute solutions of thermally stable enantiomeric molecules in achiral solvents, or even as pure molten states of such enantiomeric substances that have negligible chiral inversion rates. However, that elementary scenario is

not the primary focus of this lecture. By contrast there are known cases of relatively complex flexible molecules, not normally classified as stereochemical, whose interactions in the molten state spontaneously generate coexisting isotropic liquids of opposite chirality (handedness). The following View 2 provides the molecular structure of a nominally achiral but

---

View 2. Dressel, *et al*. molecule.

---

surely flexible organic substance, containing 138 atoms, where none of those atoms are stereocarbons. It should be mentioned that the set of mechanically stable structures for this complex flexible molecule in isolation (its individual "inherent structures") has not yet been determined, but because of the substantial number of flexibility degrees of freedom present, those stable structures presumably include several mirror-image (chiral) pairs.

The next View 3 reproduces polarized light images for a thin film of that

---

View 3. Dressel, *et al.* polarized light pictures, ambient pressure, $T = 210^{\circ}C$.

---

substance in a liquid state at ambient pressure and $T = 210^{\circ}C$. It includes a coexisting pair of immiscible phases differing only by their chirality. The liquids' isotropy property is established by showing that the relative brightness of the two regions, for a given angle between polarized light source and detector, is invariant to sample rotation. However, as shown, the relative brightness of the liquid phases will switch as that angle between source and detector changes. If the angle were exactly 90 degrees, the two liquids would be indistinguishable by brightness.

It is worth stressing that the example just shown is not unique. Other organic molecular substances with roughly comparable molecular weight and flexibility have also been demonstrated to exhibit the same spontaneous symmetry breaking that produces coexisting immiscible isotropic chiral liquids at ambient pressure.

A primary motivation for studying chiral symmetry breaking phenomena obviously emerges from terrestrial biochemistry. It is well known that the molecular building blocks of living organisms display strong chiral preferences. These substances include proteins, carbohydrates, and polynucleotides. It is generally accepted that this strong chiral bias is necessary for life as we know it to exist, to propagate, and to evolve. However it remains a fundamental mystery how the presently observed chiral bias arose, and how it has almost completely banished the mirror

image molecular competitors from living tissue. Condensed matter science has the obligation to identify and to explore all conceivable chiral symmetry breaking scenarios, to aid in ultimate identification of what actually happened geochemically as life arose on the early earth. How applicable this may be elsewhere in our universe remains an obviously tantalizing question.

The "chirality", or "handedness", of a molecule in a mechanically stable form fundamentally rests upon whether it is geometrically inequivalent to (non-superimposable with) its mirror image. The following View 4 shows

---

View 4. Alanine mirror image pairs, biological relevance of the "L" form.

---

schematically the simple specific example of the biologically relevant amino acid alanine, containing a single tetrahedral-bonding stereocarbon *C**, indicating which of its two inequivalent mirror images contributes dominantly to terrestrial living matter. With the exception of achiral glycine, the other protein-biology-relevant common amino acids also have a single α-carbon stereocenter (*C**) qualitatively in the same "L" bonding geometry as shown for alanine. The inversion barrier between L and D forms of an isolated alanine molecule has been estimated to be approximately (a) 130 kcal/mol [Lee, Shin, and Ka, Molec. Structure (Theochem) **679**, 59-63 (2004)], but more recently (b) 77.5 kcal/mol [M.E. Mohamed, Int. Lett. of Chem., Phys., and Astron. **12**, 37-44 (2013)]. Under our normal environmental circumstances chiral inversion energy barriers even roughly comparable to this range for amino acids should avoid frequent interconversion that would create biologically useless or even toxic products.

These considerations leave open the hypothetical possibility that simultaneous and complete inversion of all biomolecules in an organism and its immediate surroundings would allow it to remain alive. Amusingly, that connects to a frequently asked question about the 1871 Lewis Carroll (Charles Dodgson) novel "Through the Looking Glass", where as shown in View 5 the novel's main character Alice passes through a mirror ("reflection

---

View 5. "Through the Looking Glass" picture of Alice.

---

plane"). Have all or none of her molecules consequently undergone chiral inversion? That binary distinction will remain unanswered during the remainder of this presentation.

In order to create a tractable theoretical/simulational model for spontaneous formation of isotropic chiral liquids, emphasis needs to be

placed on a molecular geometry in three dimensions that is simpler even than those of the chiral amino acids, and is able under proper circumstances to undergo chiral inversions at a significant rate. A useful possibility is suggested by the four-atom chiral molecules hydrogen peroxide and hydrogen disulfide. Our stripped-down version is illustrated in the following View 6, which presents the two mirror-image stable structures postulated for

---

View 6. Tetramer model stable structures, mirror-image enantiomer pair.

---

the model's basic "four-monomer" tetramer. These stable structures each consist of three equal bond lengths, two 90° bond angles, and a $\pm 90^\circ$ dihedral angle. With that shape those structures each possess two-fold rotational symmetry about an axis that passes through the midpoint of the central bond. It should be stressed at the outset that this model is not intended specifically to replicate the properties of hydrogen peroxide or its sulfur analog hydrogen disulfide.

Distortions of the tetramer away from either mirror-image stable configuration raise its potential energy. The specific form chosen for the intramolecular potential energy function Φ_1 appears in the following View 7.

View 7. Tetramer model Φ_1.

It involves harmonic terms for bond length and bond angle deviations, and a non-negative trigonometric term for the dihedral angle φ. This Φ_1 form creates two distinct transition states, both planar, which can informally be denoted as an "incomplete square" (*cis*, $\varphi = 0^\circ$), and a "crankshaft" (*trans*, $\varphi = \pm 180^\circ$). They are displayed in the following View 8. These distinct

---

View 8. Two planar transition states, *cis* and *trans*.

---

transition states require the same excitation energy $K_{dih} > 0$ as specified by Φ_1. It is worth stressing that one can control thermal rates of chiral inversion in this basic model by varying this positive barrier height parameter.

The following View 9 presents a scalar chirality measure $-1 \le \zeta \le +1$

View 9. Definition of $-1 \le \zeta \le +1$

---

whose sign for a given, possibly distorted, tetramer indicates as which enantiomer it should be classified. In the case of a large number of tetramers present in a system, the respective numbers of positive (N_+) and negative (N_-) ζ's will provide the conventional enantiomeric excess "ee". Note that for any planar arrangement of the four "monomers" in a tetramer, including the two transition states, that molecule's $\zeta = 0$.

The nature of the intermolecular pair potential Φ_2 is crucial for formation of isotropic chiral liquid states. The following View 10 shows

---

View 10. Definition of tetramer pair interaction Φ_2 .

---

that it is composed of 16 Lennard-Jones (L-J) spherically symmetric terms, acting respectively between pairs of monomer sites, one on each tetramer. The key feature is that the strength of these L-J contributions depends on the product of the two chirality measures, multiplied by a coupling strength parameter $-1 < \lambda < +1$. If $\lambda > 0$, a neighboring pair of tetramers with the same chirality are favored by enhanced L-J attraction over a pair with opposite chirality. This interaction bias is reversed if $\lambda < 0$, which thus would favor neighboring pairs of tetramers having opposite chiralities. The inclusion of this renormalization chirality bias can legitimately be viewed as a coarse-grained form of chirality-sensitive intermolecular interaction, because it automatically converts each of the conventional two-center L-J interactions into eight-center interactions. No higher-order (3-tetramer, 4-tetramer, ...) molecular interactions are present in this model.

The three-dimensional continuum tetramer model just specified has been examined by molecular dynamics simulation (via the LAMMPS software package), for both signs of the chirality biasing parameter λ. In order to keep the simulation investigation within reasonable bounds, the other interaction parameters have been confined to a fixed set of dimensionless values shown in the following View 11. In case one might be interested,

---

View 11. Φ_1 and Φ_2 interaction parameters, in reduced units. Also physical unit values assigned roughly by H_2O_2 .

View 11 also presents parameter values converted to corresponding physical dimensions, using monomer magnitudes roughly consistent with the model-motivating real substance hydrogen peroxide.

At least under moderate external pressure conditions, the fluid and crystal phases for $\lambda < 0$ are found to be racemic ($< \zeta >= 0$, $ee = 0$) as expected. However when $\lambda > 0$, we observe that under isochoric (constant *N*/*V*) conditions, cooling of an initially hot racemic fluid experiences phase separation into immiscible isotropic chiral liquids. This latter phase change behavior is illustrated by the following simulation results, in which the two tetramer chiralities are shown as red and blue, respectively. First, View 12

View 12. $N/V = 0.17$, $T = 4.0$, $\lambda = +0.5$, $N = 1024$, rapid melting and racemization of the initial configuration, monitored by time dependence of $< \zeta >$.

---

confirms the relevance of uniform racemization at high temperature, showing rapid kinetic degradation of an initial pure-chirality spatially ordered configuration to a statistically persistent racemic fluid. By contrast, the following View 13 involves the same number of tetramers (1024) and

---

View 13. $N/V = 0.17$, $T = 1.4$, $\lambda = +0.5$, $N = 1024$, phase separation into coexisting isotropic chiral liquids from a racemic initial condition.

---

number density (0.17) as in the preceding View 12, but at a substantially lower reduced temperature $T = 1.4$. Its initial condition is a racemic configuration taken from the late stage of the high temperature simulation in View 12. A pair of side-by-side liquids with opposite mean chirality spontaneously appears, both of which are isotropic (no liquid-crystal type long-range order). Because the contact interface between these phases is expected, and appears, to have positive free energy (positive surface tension), a thermodynamic driving force ultimately would have one of the two phases dominate (*i.e.,* consume) the other. However that would be a very slow process at the prevailing simulation temperature, as indeed was the case for the experimental system shown earlier.

If the same molecular dynamics run shown in View 13 had been performed, except with the opposite assignment $\lambda = -0.5$, the racemic state would have persisted over the entire simulation time interval.

Based on several molecular dynamics runs of the types just illustrated in the last two Views, 12 and 13, a broader picture of this spontaneous chiral symmetry breaking phenomenon for $\lambda > 0$ appears in the following View 14.

View 14. Equilibrated isochoric *T* dependence of $< \zeta >$, $\lambda \approx +0.5$.

$T_c(\langle\zeta\rangle) \approx 2.5$.

This schematically indicates the pattern of full isochoric temperature dependence of $\langle\zeta\rangle$ for a liquid-density system, including the expected low temperature freezing of the isotropic chiral liquids at $T_m > 0$ (with crystallography to be examined a bit later). For now, attention needs to be focused on the existence of a critical point resulting from the model's $\lambda > 0$ chiral symmetry breaking phenomenon. This is strongly analogous to the more familiar liquid-vapor critical point, or to phase separation of a binary liquid solution. Indeed it may be described with the same critical exponent values for analogous properties. The most obvious critical singularity exponents are those describing *T* dependence of the coexistence curve shape ($\beta \cong 0.326$), and of the liquid-liquid interfacial tension ($\mu \cong 1.26 \cong 5/4$). The critical temperature will of course depend on the number density, and on the specific positive value assigned to the renormalization parameter λ. Simulations for the preceding case $\lambda = +0.5$ and $\rho = 0.17$ illustrated earlier in Views 12 and 13 produced an estimated $T_c(\langle\zeta\rangle) \approx 2.5$.

No analog for that chiral symmetry-breaking critical point in the liquid phase will occur for $\lambda < 0$, at least under moderate density or pressure. If $|\lambda|$ were small however, the L-J interactions would still provide roughly comparable attractive interactions between all pairs of tetramers, giving rise to a conventional liquid-vapor critical point. In that alternative critical state the system's number density is fixed, in contrast to the chiral symmetry breaking critical phenomenon which can occur over a non-zero range of number densities. This leads to the intriguing possibility that certain specific choices of the model's interaction parameters can produce both kinds of critical points. The next View 15 presents a schematic isochoric view of the

---

View 15. Thermal equilibrium contours for a modest $\lambda > 0$ representing the compositions of the coexisting uniform phases within $<\zeta>$, ρ, T space, and showing the presence of two distinct critical points. Here the overall system density is isochoric, fixed at $\rho = \rho_c(l,v)$, and $T_c(l,v) > T_c(\langle\zeta\rangle)$.

---

thermal equilibrium state loci for the uniform phases expected to coexist in such a circumstance, specifically requiring a modest $\lambda > 0$. Here the fixed value of liquid-vapor critical density applies for the entire closed system, represented in the three-dimensional $<\zeta>$, ρ, T space. It clearly indicates

the two distinct critical temperatures $T_c(l,v)$ and $T_c(\langle\zeta\rangle)$. Under the enforced isochoric condition, only the coexistence-separated dense liquid phase is subject to the chiral symmetry breaking phenomenon at the lower critical temperature $T_c(\langle\zeta\rangle)$.

Note that the two-critical-point scenario just described involves three distinct fluid surface tensions. These are associated with: (1) the vapor-racemic liquid interface in the temperature range $T_c(l,v) > T \geq T_c(\langle\zeta\rangle)$; (2) the vapor-isotropic chiral liquid interface for $T_c(\langle\zeta\rangle) \geq T \geq T_m$; and (3) the coexistence contact interface for the opposite-chirality isotropic liquids, also in the temperature range $T_c(\langle\zeta\rangle) \geq T \geq T_m$. It remains to be determined if interface cases (1) and (3) exhibit the usually measured surface tension temperature-dependence exponent value $\mu \cong 1.26 \cong 5/4$ for critical regions.

By altering the various parameters contained in Φ_1 and Φ_2 it should be possible to change the relative temperatures of the two critical points in an isochoric plot of the sort just displayed. A special circumstance that could conceivably arise is confluence of the two critical points. This would be expected to occur upon increasing the magnitude of the positive renormalization parameter λ. View 16 indicates qualitatively how the same

---

View 16. Same type of schematic as View 15, except for confluence of critical points, $T_c(l,v) = T_c(\langle\zeta\rangle)$.

---

kind of three-dimensional plot just shown in the preceding View 15 would be modified if this confluence were to occur. Note that in this unusual circumstance there would be three homogeneous phase property curves emanating downward from the joint critical point, rather than two. However, now there would be only two distinct interfacial surface tensions: (1) chiral-liquid, racemic-vapor case, and (2) coexistence contact between the opposite chirality isotropic liquids.

It is worth mentioning that the chiral-symmetry-breaking critical point could in principal rise in temperature above this confluence. However, upon doing so it would eliminate appearance of the full liquid-vapor critical point region, leaving just a portion of the racemic vapor phase curve in an isochoric plot. This seems unlikely for the tetramer model under consideration, with physically sensible parameter assignments.

The tetramer pair interactions that produce spontaneous chiral symmetry breaking in the liquid phase are the basic determinants of the corresponding low temperature crystal structures. In order to attain a comprehensive

understanding of the tetramer model, some effort has also been directed toward discovering the ground-state ($T = 0$) crystals for various values of the renormalization parameter λ, at least for low to moderate pressures. The technique used for this task is a "genetic algorithm". View 17 illustrates

---

View 17. Racemic crystal structure for:

$$\lambda = -0.50,\ T = 0,\ \rho = 0.24,\ \phi = -30.35,\ p \approx 0\ .$$

Bravais lattice type: triclinic.

---

a racemic crystal case, which has two tetramers per unit cell, one of each handedness. The following View 18 provides a corresponding enantiopure

---

View 18. Enantiopure crystal structure for:

$$\lambda = +0.50,\ T = 0,\ \rho = 0.24,\ \phi = -40.28,\ p \approx 0\ .$$

Bravais lattice type: triclinic.

---

crystal structure where the sign of renormalization parameter λ has been reversed. Again the unit cell contains two tetramers, now obviously with the same handedness. Both structures 17 and 18 are triclinic.

The tetramer model presented here deserves a lot of additional quantitative study, both analytical and simulational. But it is also valuable to postulate qualitatively what extensions and other kinds of three-dimensional continuum models would be worth constructing and pursuing. The last View 19 lists several intriguing possibilities.

View 19. Extensions to different three-dimensional continuum models to investigate chiral symmetry breaking phenomena. Flexible molecules that are nominally achiral (*i.e.*, Dressel, *et al.*). Several stereocenters. Liquid crystals. Generalization of ζ for stereocarbon cases. Influence of achiral solvents.

View 1
(click to go back)

Chiral Symmetry Breaking in Isotropic Liquids

Frank H. Stillinger
Dept. of Chemistry, Princeton University
Princeton, NJ 08544

Research collaborators:

Folarin Latinwo and Pablo Debenedetti
Dept. of Chemical and Biological Engineering
Princeton University, Princeton, NJ 08544

Arash Nikoubashman
Institute of Physics, Johannes Gutenberg University Mainz
Staudingerweg 7, 55128 Mainz, Germany

View 2
(click to go back)

Immiscible Pairs of Isotropic Chiral Liquids

Reference:

C. Dressel, T. Reppe, M. Prehm, M. Brautzsch, and C. Tschierske, *Nature Chemistry* **6**, 971-977 (2014), "Chiral self-sorting and amplification in isotropic liquids of achiral molecules".

Molecular structure (R = *n* - C_6H_{13}):

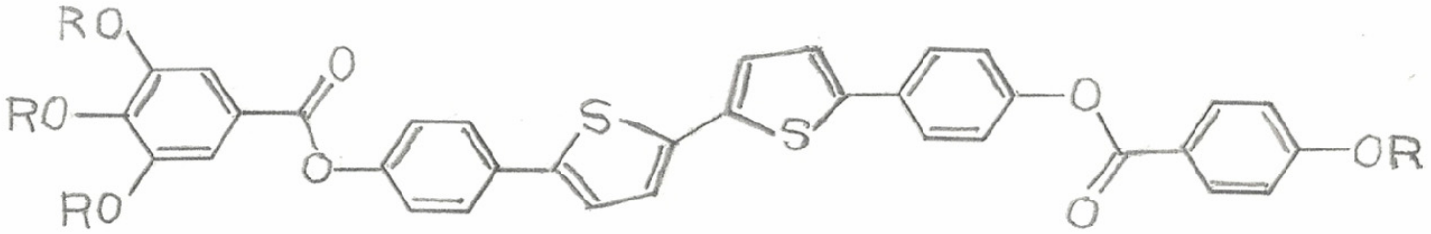

Approximate temperature range of immiscibility: $177^\circ C \leq T \leq 213^\circ C$

View 3
(click to go back)

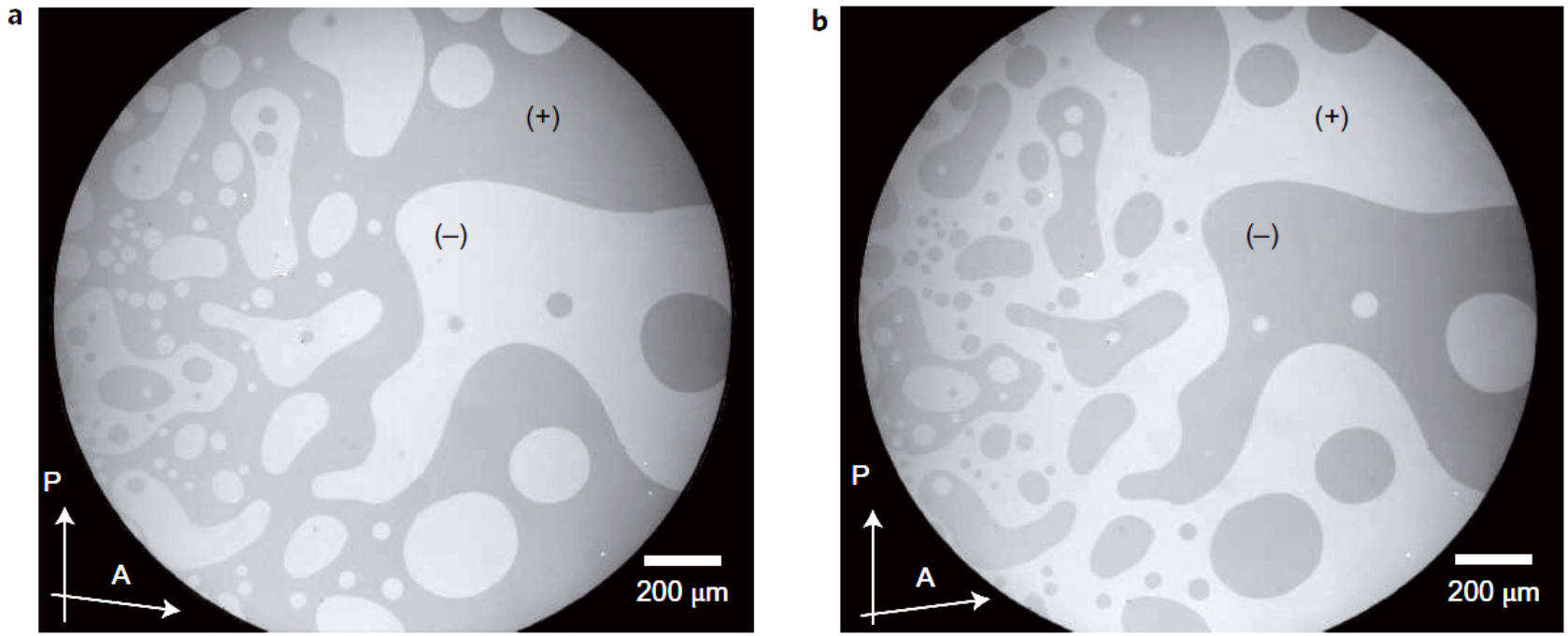

View 4
(click to go back)

AMINO ACID EXAMPLE: ALANINE

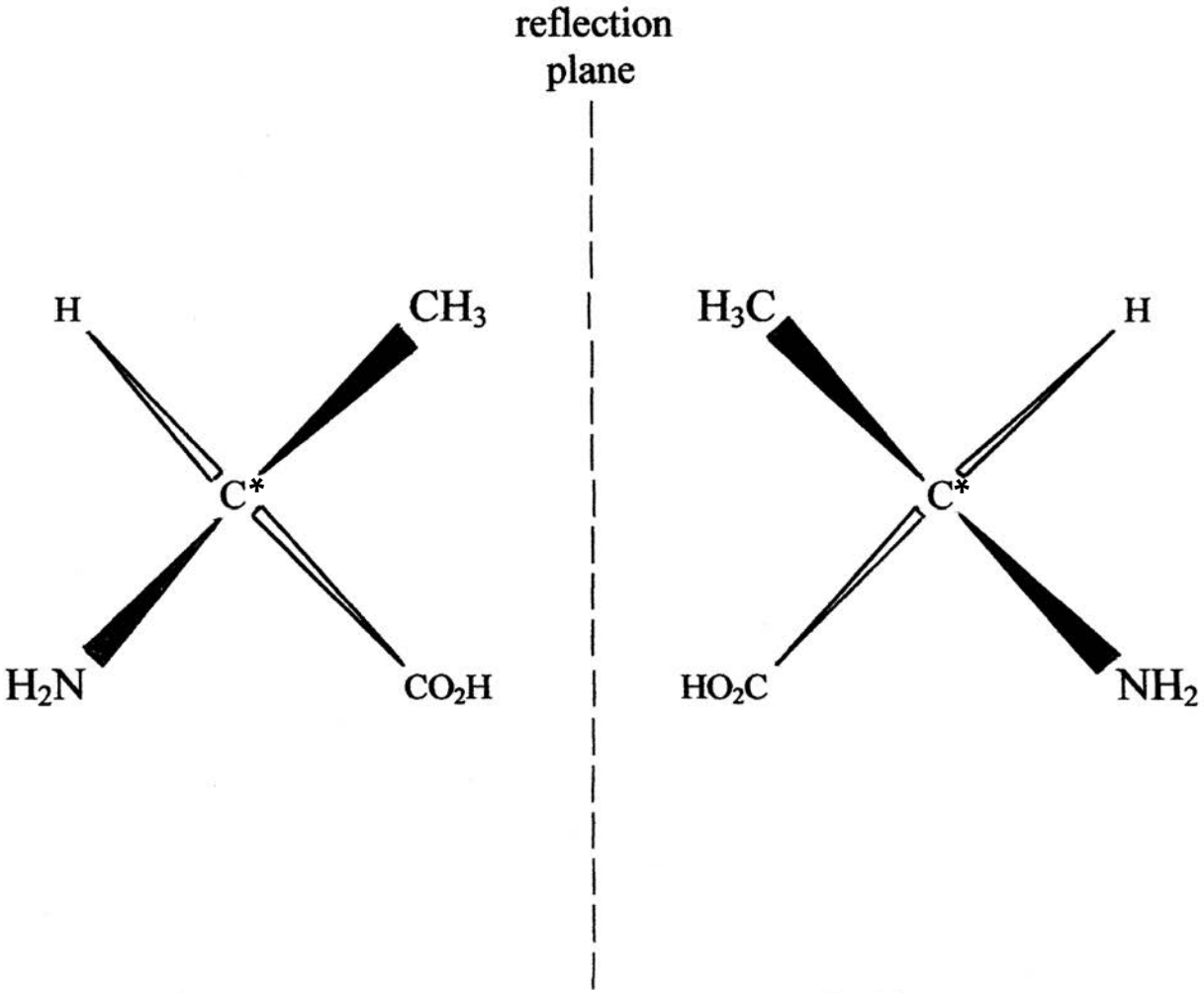

"L" isomer

biologically favored

"D" isomer

View 5
(click to go back)

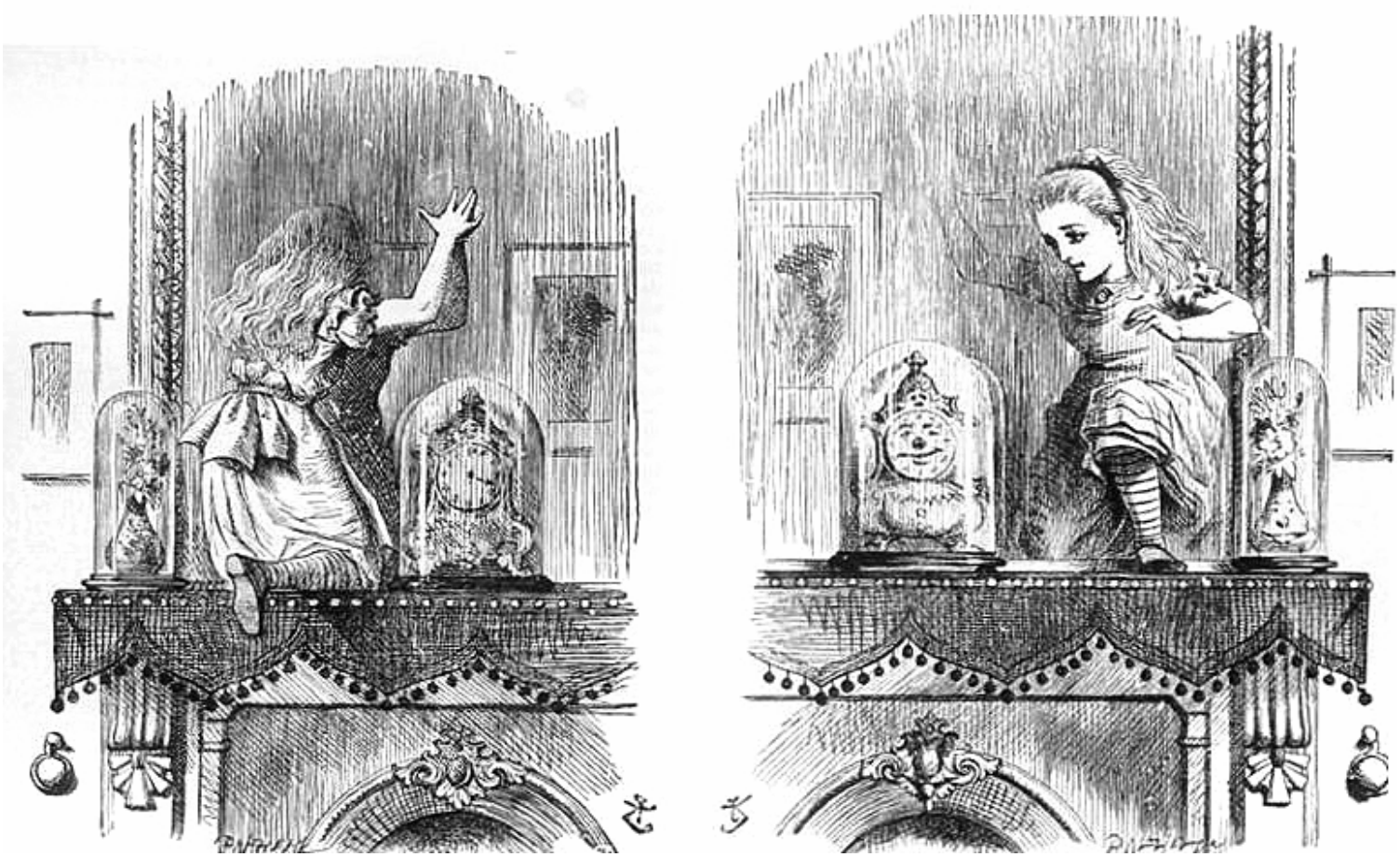

View 6
(click to go back)

Flexible Tetramer Model, Stable Structures

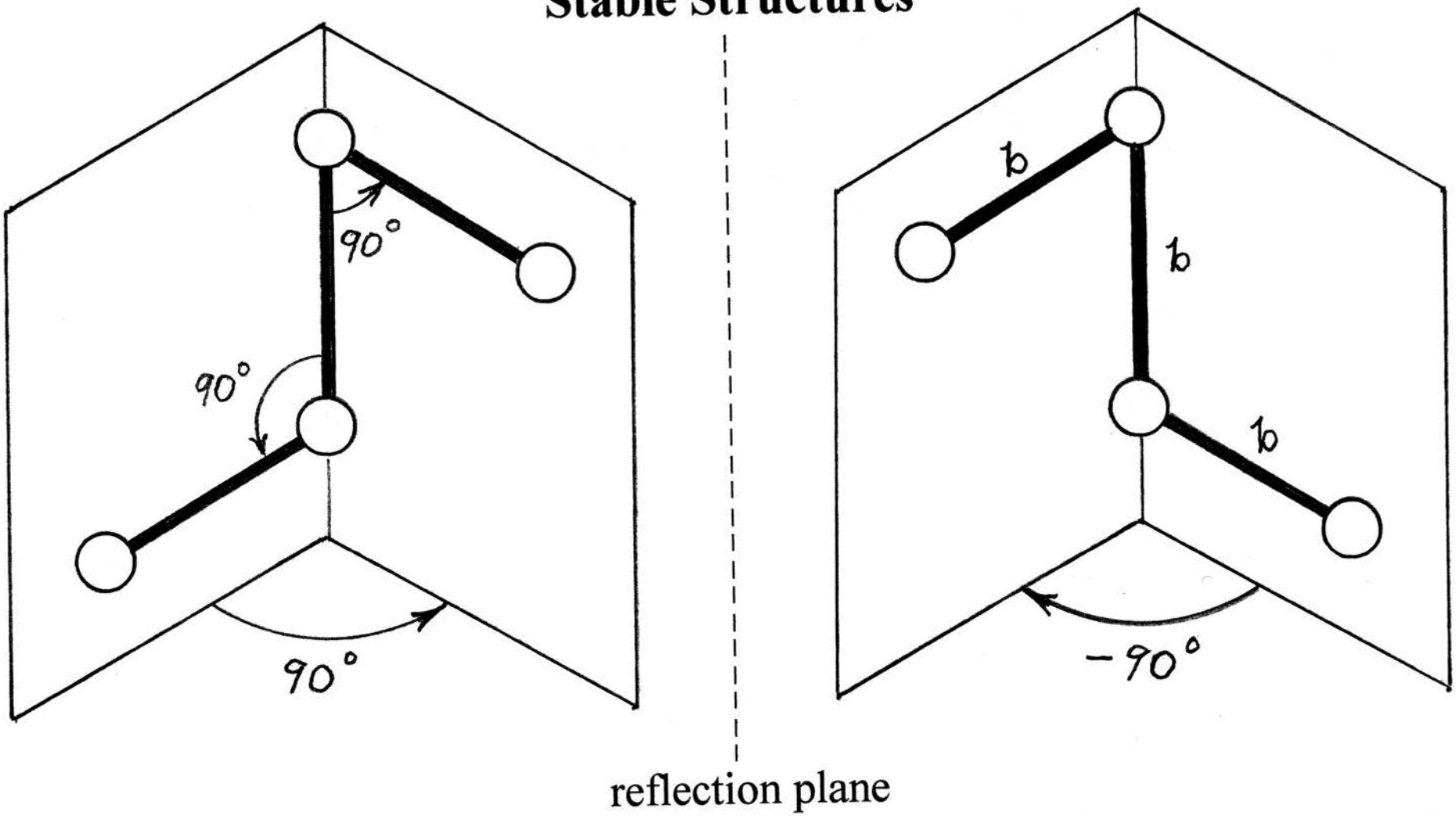

View 7
(click to go back)

Tetramer Intramolecular Potential Energy

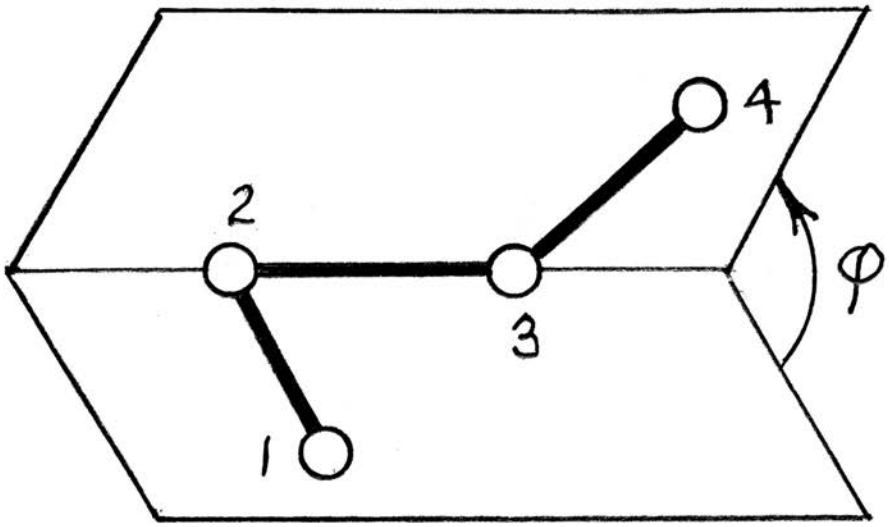

$$\Phi^{(1)}(\mathbf{r}_1,\mathbf{r}_2,\mathbf{r}_3,\mathbf{r}_4) = \sum_{i=1}^{3}(K_{str}/2)(r_{i,i+1}-b)^2 + \sum_{i=2}^{3}(K_{bnd}/2)(\theta_i-\pi/2)^2 + K_{dih}\cos^2\varphi \quad .$$

Dihedral angle $-\pi \le \varphi \le \pi$ definition:

$$\cos\varphi = \frac{(\mathbf{r}_{12}\times\mathbf{r}_{23})\cdot(\mathbf{r}_{23}\times\mathbf{r}_{34})}{|\mathbf{r}_{12}\times\mathbf{r}_{23}||\mathbf{r}_{23}\times\mathbf{r}_{34}|} \quad .$$

Distinct Planar Transition States, Isolated Tetramer

- $\varphi = 0$:

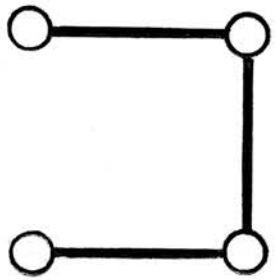

- $\varphi = \pm\pi$:

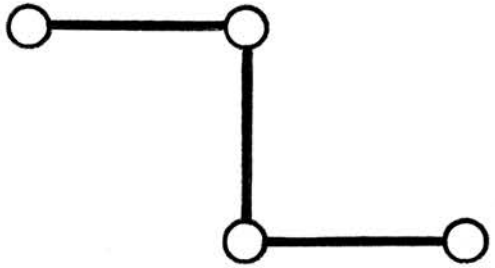

- Transition state barrier height: K_{dih}

- Harmonic normal mode frequencies at each transition state:
  five positive, six vanishing, one imaginary (reaction path)

Chirality Measure for Individual Tetramers

- Monomers located at $\mathbf{r}_1, \mathbf{r}_2, \mathbf{r}_3, \mathbf{r}_4$.
- $\zeta(\mathbf{r}_1,\mathbf{r}_2,\mathbf{r}_3,\mathbf{r}_4) = \dfrac{\mathbf{r}_{12}\cdot(\mathbf{r}_{23}\times\mathbf{r}_{34})}{|\mathbf{r}_{12}||\mathbf{r}_{23}||\mathbf{r}_{34}|} \equiv \dfrac{\mathbf{r}_{43}\cdot(\mathbf{r}_{32}\times\mathbf{r}_{21})}{|\mathbf{r}_{43}||\mathbf{r}_{32}||\mathbf{r}_{21}|}$.
- $-1 \le \zeta \le +1$; $\zeta = \pm 1$ at the $\Phi^{(1)}$ minima .
- $\zeta = 0$ for tetramer planar configurations, including the ideal transition states.
- Enantiomeric excess ("ee"): $-1 \le (N_+ - N_-)/(N_+ + N_-) \le +1$

Tetramer Pair Interaction ($\Phi^{(2)}$)

- Sixteen energy-scaled Lennard-Jones pair interactions between monomers belonging to different tetramers (α, γ):

$$\Phi^{(2)} = \sum_{i=1}^{4}\sum_{j=1}^{4} \varepsilon_{mm}(\zeta^{(\alpha)},\zeta^{(\gamma)})\, v_{\mathrm{LJ}}(|\,\mathbf{r}_i^{(\alpha)} - \mathbf{r}_j^{(\gamma)}\,|/\sigma_0) \quad .$$

- $v_{\mathrm{LJ}}(x) = 4(x^{-12} - x^{-6})$.

- $\varepsilon_{mm}(\zeta^{(\alpha)},\zeta^{(\gamma)}) = \varepsilon_0(1 + \lambda\zeta^{(\alpha)}\zeta^{(\gamma)})$, where $|\lambda| < 1$.

- $\lambda > 0$ favors like enantiomers, $\lambda < 0$ favors opposite enantiomers.

- ε_{mm} varies smoothly as the tetramers deform, passing through ε_0 when one tetramer changes chirality.

View 11
(click to go back)

Parameter Choice, Reduced Units

- Elementary parameter set choice: m, ε_0, σ_0
  $[m = 8.5\text{g/mol};\quad \varepsilon_0 = 0.15535\text{kcal/mol};\ \sigma_0 = 1.115\,\text{Å}]$

- Time unit: $\sigma_0 (m/\varepsilon_0)^{1/2}$ $[\rightarrow 0.4033\,\text{ps}]$

- Number density unit: σ_0^{-3} $[\rightarrow 0.7214\,\text{Å}^{-3} = 1198\,\text{mol/l}]$

- Temperature unit: ε_0 / k_B $[\rightarrow 78.15\,\text{K}]$

- Pressure unit: $\varepsilon_0 / \sigma_0^3$ $[\rightarrow 7786\,\text{bar}]$

- Dimensionless intramolecular ($\Phi^{(1)}$) parameters:

$$K_{str} = 8003, \quad K_{bnd} = 643.7, \quad K_{dih} = 17.86, \quad b = 1.0583$$

View 12
(click to go back)

Time dependence of average chirality at high temperature, T= 4.0
(reduced tetramer number density = 0.17)

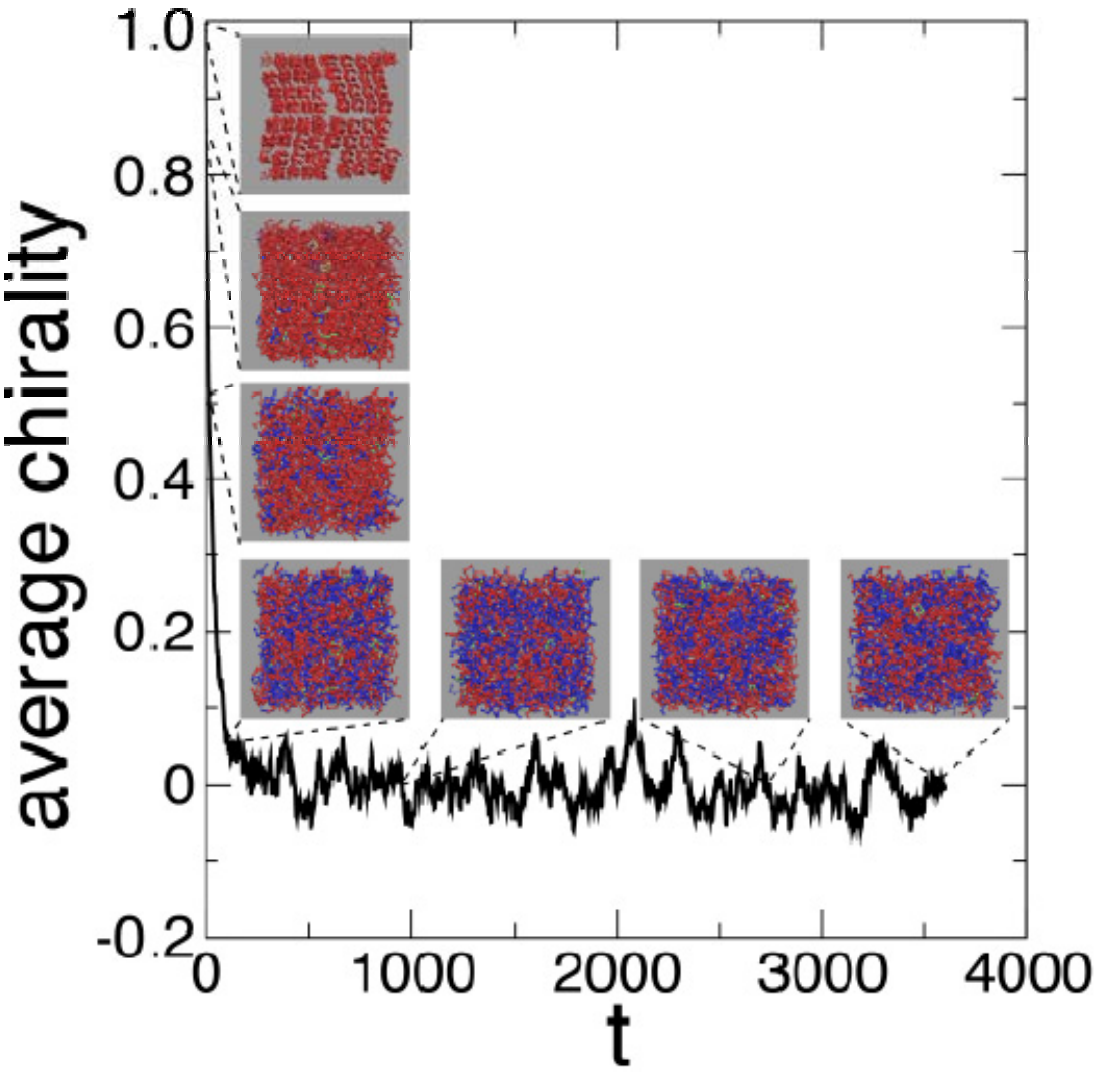

View 13
(click to go back)

Chirality-induced liquid-liquid phase separation

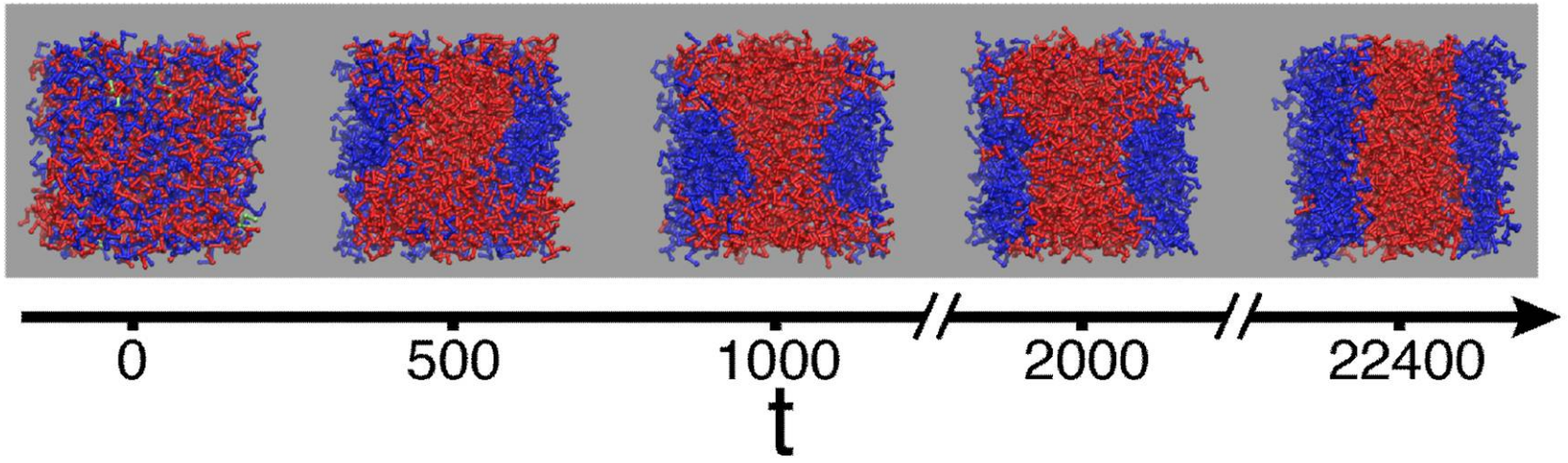

View 14
(click to go back)

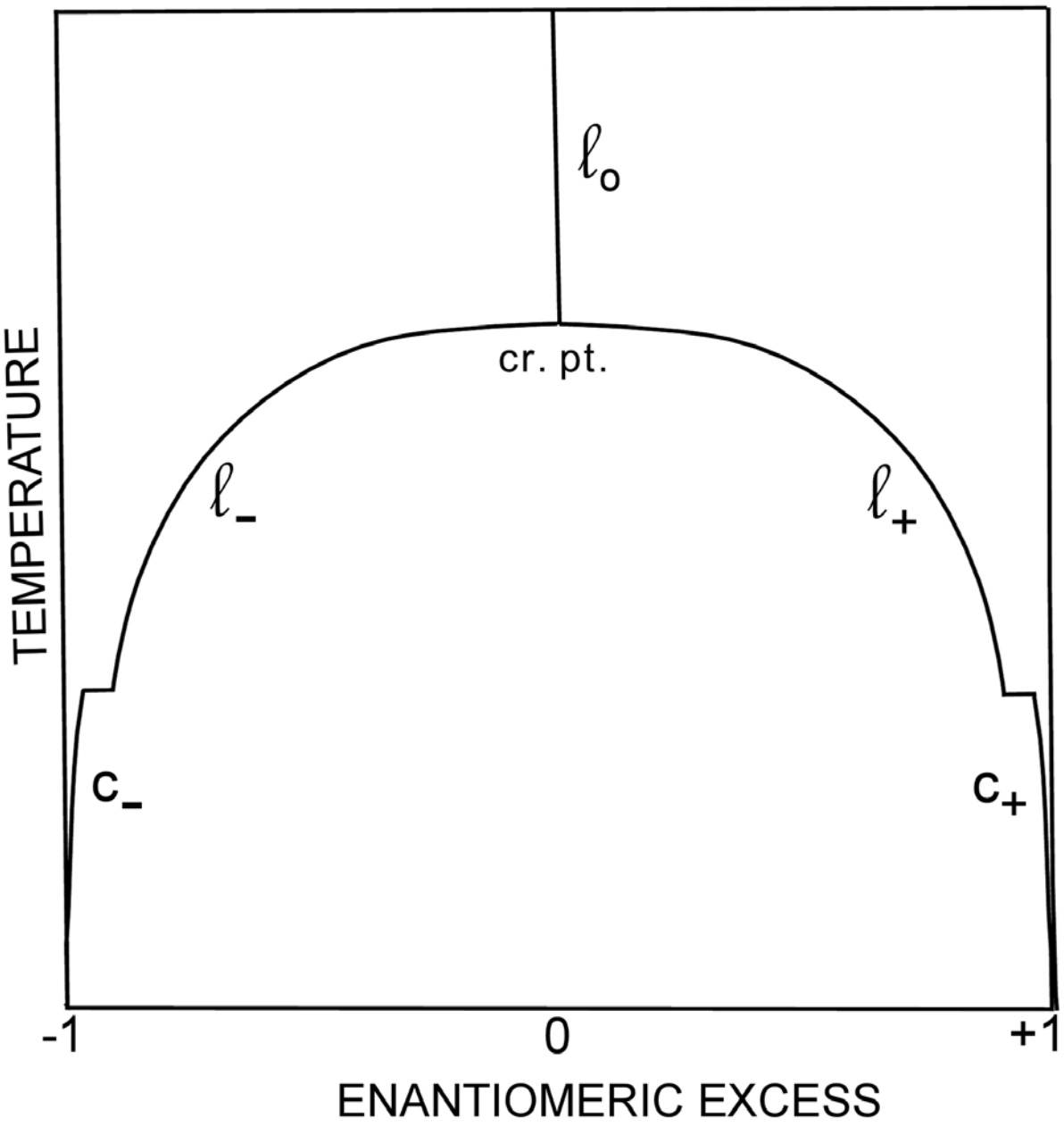

View 15
(click to go back)

Distinct Critical Points: $T_c(liq-vap) > T_c(chirality)$

[isochoric conditions: $\rho = \rho_c(liq-vap)$]

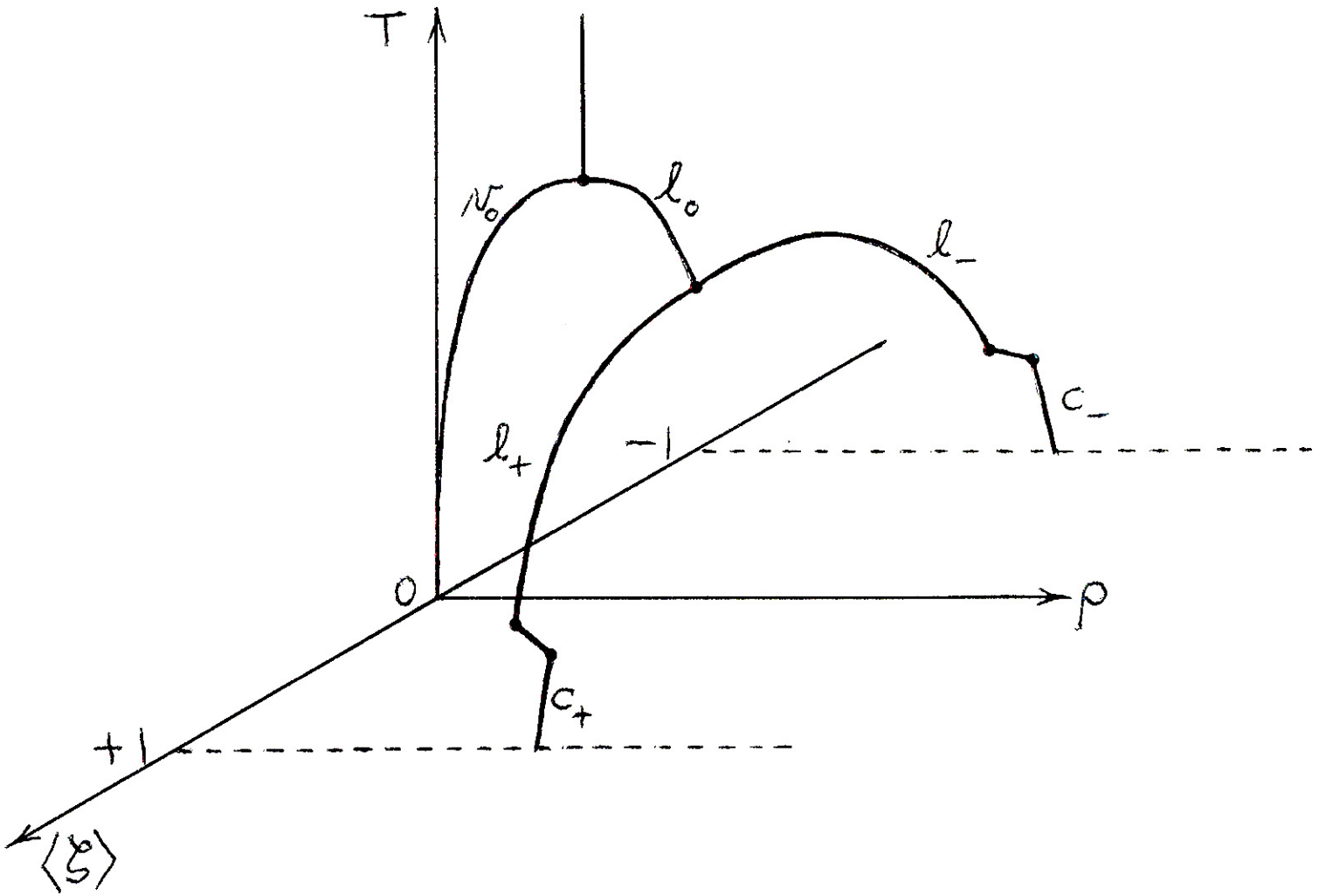

View 16
(click to go back)

Confluent Critical Points: $T_c(liq-vap) \equiv T_c(chirality)$

[isochoric conditions: $\rho = \rho_c(liq-vap) \equiv \rho_c(chirality)$]

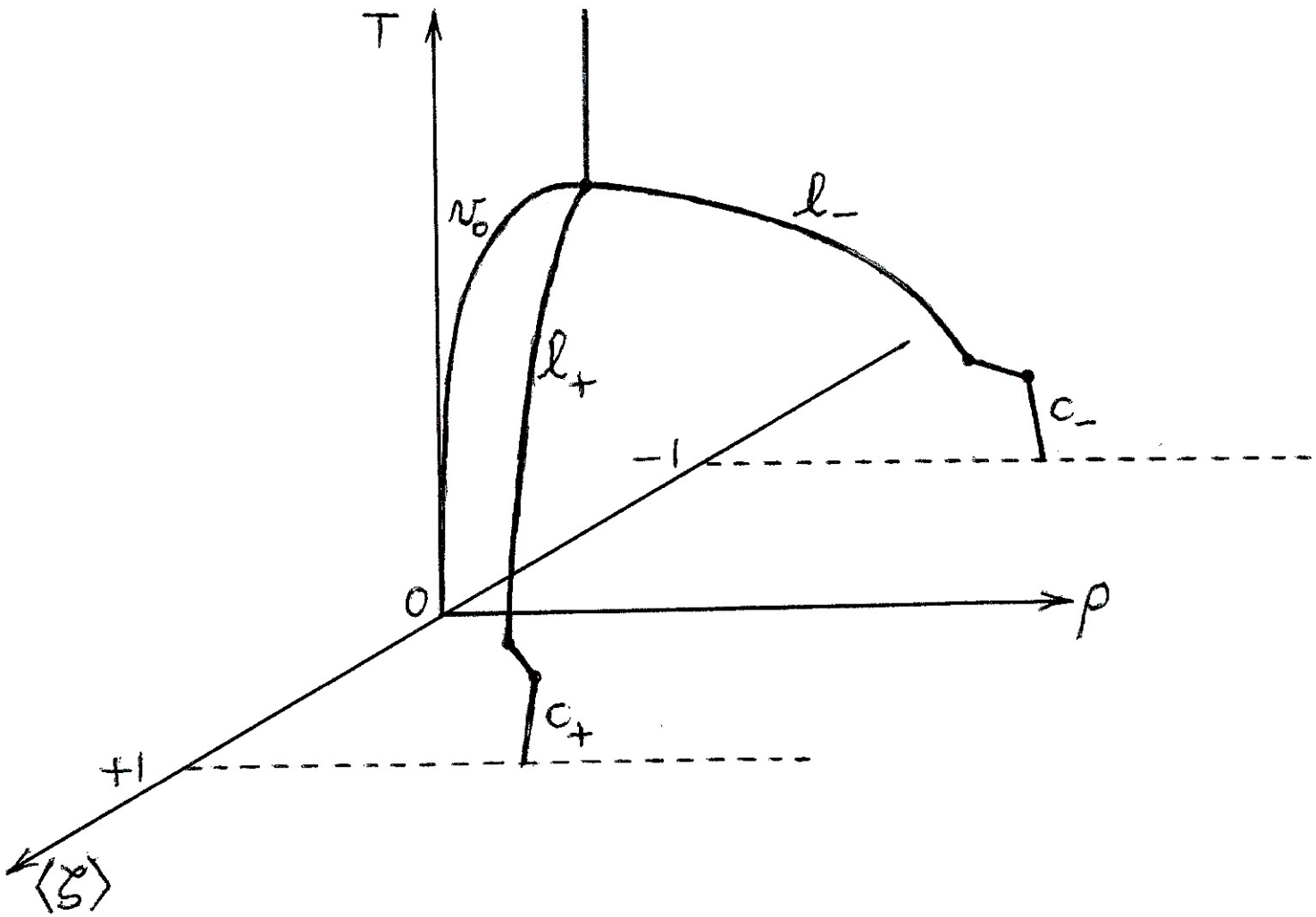

View 17
(click to go back)

Most Stable Racemate

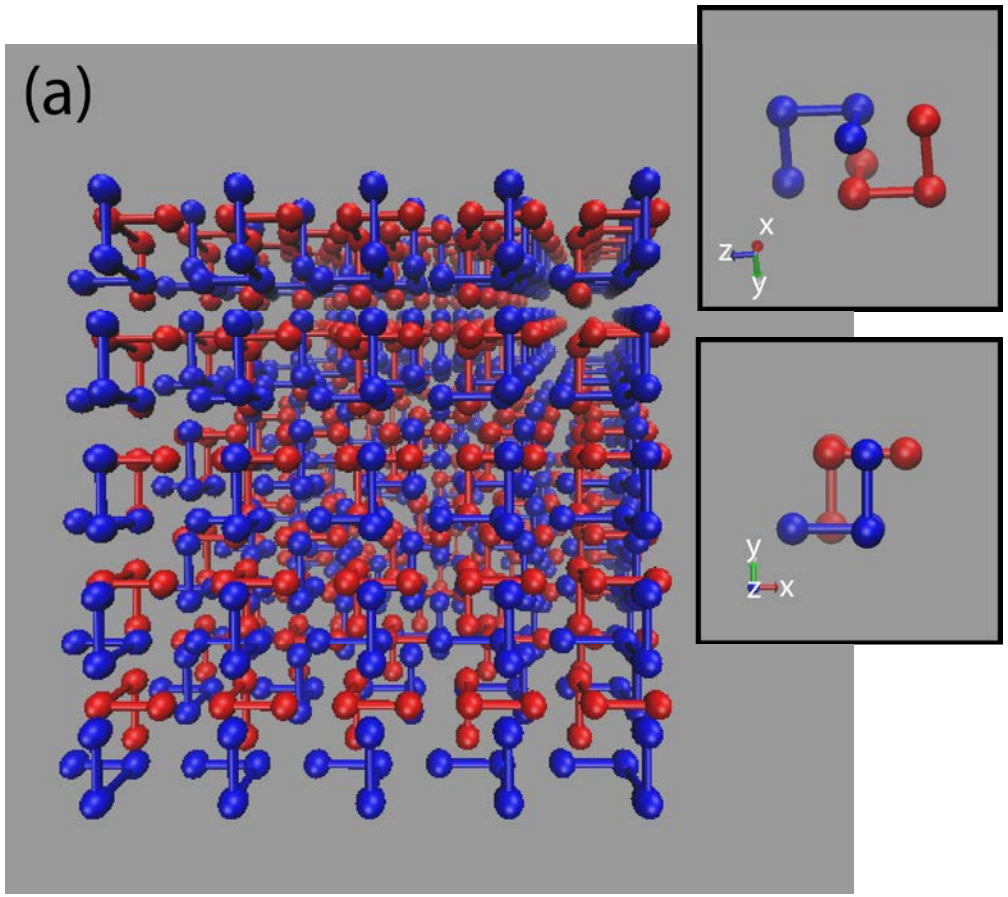

$$(\lambda, \rho) = (-0.5, 0.24)$$

$$\phi = -30.3527$$

$$a = 2.0834$$

$$b = 2.0812$$

$$c = 2.0797$$

$$\alpha = 106.36^{\circ}$$

$$\beta = 105.12^{\circ}$$

$$\gamma = 89.36^{\circ}$$

250 molecules shown

View 18
(click to go back)

Most Stable Conglomerate

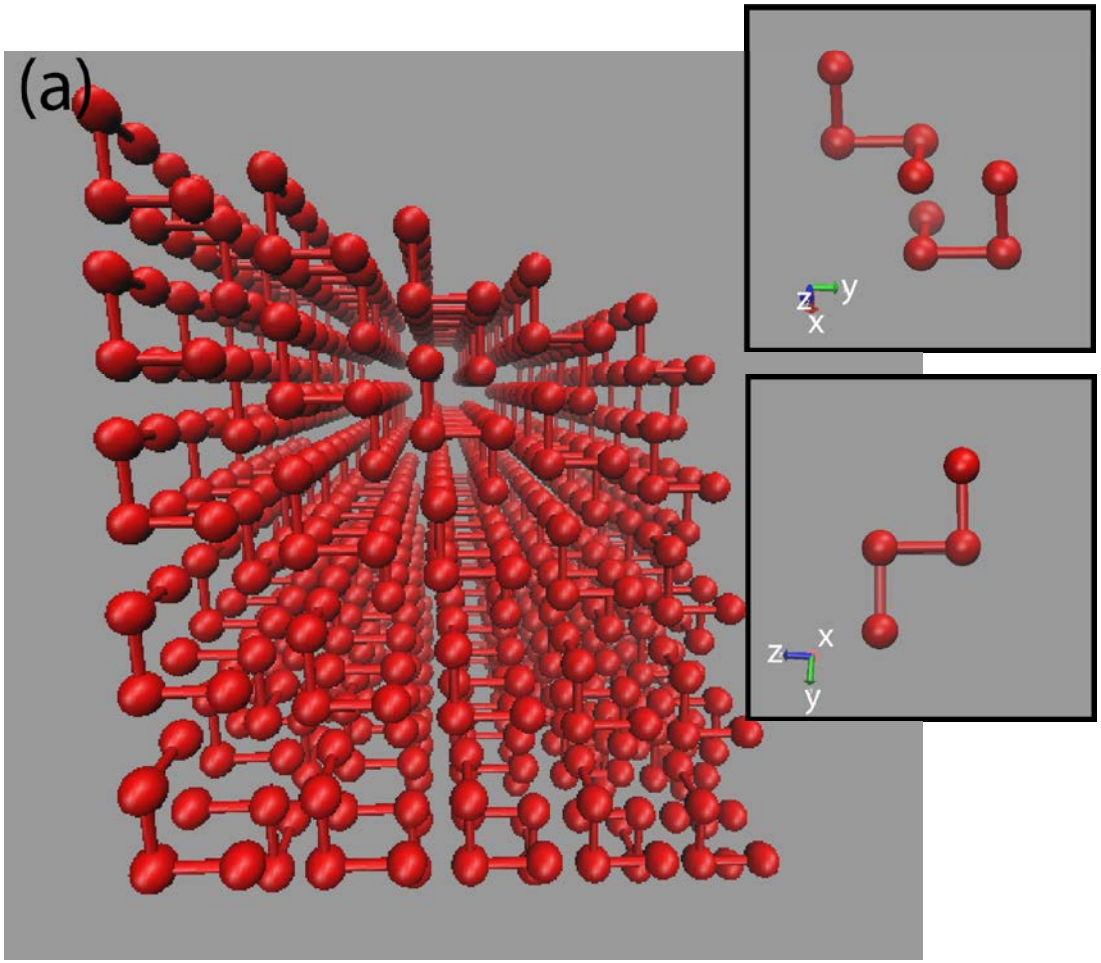

250 molecules shown

$$(\lambda, \rho) = (0.5, 0.24)$$

$$\phi = -40.2844$$

$$a = 2.1850$$

$$b = 2.1078$$

$$c = 2.0721$$

$$\alpha = 74.89^\circ$$

$$\beta = 74.97^\circ$$

$$\gamma = 105.02^\circ$$

View 19
(click to go back)

Additional Research Opportunities

- Calculation of optical rotation for many-tetramer systems where individual tetramer polarizability has been defined.

- Tetramer model response to an external field with potential energy proportional to $\sum \zeta_j$.

- Construction and investigation of a simple stereocarbon model

- Create a three-dimensional continuum model that produces chiral product molecules from achiral reactants.